Alfarama Journal of Basic & Applied Sciences

https://ajbas.journals.ekb.eg
ajbas@sci.psu.edu.eg

Faculty of Science Port Said University

http://sci.psu.edu.eg/en/

October 2024, Volume 5, Issue IV (Special Issue)

DOI:**https://doi.org/10.21608/AJBAS.2024.304517.1219**

ISSN 2682-275X

Submitted: 15/07/2024
Accepted: 27/08/2024

Pages: 561 - 572

Three-dimensional nonlinear ion-acoustic solitary waves in the Venusian ionosphere at high altitude

B. M. Farouk[1,*], A. Atteya[2], M. El-Metwally[1], and W. M. Moslem[1, 3]

[1] Department of Physics, Faculty of Science, Port Said University, Port Said P.O 42521, Egypt

[2] Department of Physics, Faculty of Science, Alexandria University, Alexandria, P.O. 21511, Egypt

[3] Centre for Theoretical Physics, The British University in Egypt (BUE), El-Shorouk city, Cairo, Egypt

*** Correspondence author:** belal.farouk@sci.psu.edu.eg

ABSTRACT

After Earth, Venus has been the planet in our solar system most extensively explored. Solitary and double layers of plasma waves were found in the Venusian environment by analysis of the data provided by satellite observations (e.g., Venera, Mariner, Pioneer Venus Orbiter, and Venus Express). We investigate three-dimensional nonlinear electrostatic ion-acoustic waves (IAWs) between 10^3 and 10^4 km above the surface of Venus in a homogeneous, collisionless, unmagnetized plasma environment. Together with Maxwellian electrons from Venus, the plasma system under investigation contains two kinds of positively charged planetary ions, namely H^+ and O^+. Solar wind Maxwellian electrons and flowing protons are other interactions with this system. We derive the suitable evolution equation, the Kadomtsev-Petviashvili (KP) equation, to model three-dimensional nonlinear ion acoustic solitary wave propagation. An essential part of explaining the development of the nonlinear wave phenomena in our plasma system is played by this equation. We applied an energy consideration-based approach to ascertain the stability of the solitary waves. With this method, we may ascertain if the solitary wave characteristics stay constant, during propagation, which advances our knowledge of wave behavior dynamics in three dimensions. Using energy-based analysis, we study the prerequisites for the stability and development of solitary waves. The stability of localized structures with transverse direction fluctuations is investigated. The wave propagation is studied at various altitudes in connection with the physical properties of the plasma in the Venusian ionosphere. This research enhances our understanding of ion-acoustic solitary waves within the plasma environment of Venus while also contributing to our broader knowledge of wave propagation mechanisms in space plasma.

Key Words: Venus ionosphere; ion-acoustic waves; high altitude; Kadomtsev-Petviashvili KP equation; soliton; solar wind; plasma waves.

1. INTRODUCTION

Space physics depends on our ability to comprehend the nonlinear processes that occur in the planet's ionosphere. The characteristics of the planetary blockage and the attributes of different plasma parameters affect these nonlinearities [1]. Based on observations, the solar wind, which is an extension of the solar corona, at 1 AU (AU is the Sun-Earth distance), has a typical ion number density of about 7 cm^{-3} and consists of approximately 95% protons and 5% helium, with other minor ions [2]. The interaction between the solar wind and planetary environments is determined by plasma properties, electromagnetic surroundings, and solar activity [3, 4]. The solar wind releases approximately 10^{12} g/s or one million metric tons of charged particles per second into space, with energy levels ranging from 1.5 to 10 keV and speeds ranging from 250 to 750 km/s [5]. Venus, Earth's enigmatic twin, features a dense, turbulent atmosphere and lacks a global magnetic field [6]. Exposed directly to the solar wind, Venus's ionosphere undergoes unique dynamics that shape its composition and density, influencing its surface protection and temperature regulation [7, 8].

Although all rocky terrestrial planets, Mercury, Venus, Earth, and Mars, respond differently to solar wind [9], Earth and Mercury have intrinsic magnetic fields that shield them from direct solar wind exposure. In contrast, Venus and Mars lack such fields, exposing their atmospheres to direct solar wind interactions [10]. Planets with magnetic fields form magnetosphere cavities with extended tails, while those without generate magnetospheres through electric currents in their ionospheres. These variations are influenced by each planet's distance from the sun and fluctuations in solar radiance and wind properties [11].

We can learn more about solar-planetary interactions and planetary ionospheres by studying Venus's plasma dynamics, which helps us find livable worlds outside of our solar system. Venus is therefore a subject of great scientific interest and the target of multiple space missions [12]. Venus's plasma has been investigated by several missions [13]. Despite instrumentation limitations, the Pioneer Venus Orbiter (PVO) was the first long-term orbiter dedicated to these investigations, contributing to our understanding of Venus's induced magnetosphere. Important data were obtained [14] from the ASPERA-4 Ion Mass Analyzer on Venus Express (VEX), which advanced our understanding of ionospheric ions and plasma flow. Venus does not have an internal magnetic dynamo, as proven by PVO's magnetometer data [15]. Venus's ionospheric ion composition is still being measured by ASPERA-4 [16]. Much recent work has been devoted to studying single waves near Venus's plasma boundary. A thorough description of the electrostatic ion-acoustic waves (IAWs) seen in different Venusian plasma settings is provided by Yadav (2020) [12].

Our goal in this work is to further understand possible nonlinear waves in the Venusian ionosphere at high altitudes between 10^3 and 10^4 km while accounting for the effect of the streaming solar wind. Our system encompasses two positively charged planetary ions, H^+ and O^+ from Venus, along with isothermal electrons and streaming solar wind (SW) protons, accompanied by Maxwellian electrons. By employing reductive perturbation analysis, we derived the three-dimensional Kadomtsev-Petviashvili KP equation to depict the dynamics of weakly nonlinear electrostatic ion-acoustic waves (IAWs) within the Venusian ionosphere at altitudes spanning 10^3 to 10^4 km. In order to assess the stability of isolated waves, we utilized an energy consideration method. This technique advances our knowledge of the dynamics of wave behavior in three dimensions by allowing us to ascertain if the properties of solitary waves remain consistent during propagation [17].

2. Plasma model

Our investigation focuses on the propagation of three-dimensional (3D) nonlinear electrostatic ion-acoustic waves (IAWs) in an unmagnetized plasma environment, characterized by uniformity and the absence of collisions. This plasma medium comprises two planetary ions, H^+ and O^+, originating from Venus, along with isothermal electrons, solar wind (SW) protons, and solar wind electrons, denoted by subscripts H, O, e, sp, and se, respectively [18]. Our system is designed to have cold plasma, which means that the temperature of the ions will be much lower than the effective temperature, $T_{ion} \ll T_{eff}$, and finally, it will approach zero. The resultant normalized continuity and momentum equations governing the dynamics of these waves in the plasma system are provided by:

For H^{+},

$$\frac{\partial \mathrm{n_H}}{\partial \mathrm{t}} + \boldsymbol{\nabla} \mathrm{n_H} \mathbf{u}_\mathrm{H} = 0, \tag{1a}$$

$$\frac{\partial \mathbf{u}_\mathrm{H}}{\partial \mathrm{t}} + (\mathbf{u}_\mathrm{H}.\boldsymbol{\nabla})\mathbf{u}_\mathrm{H} + \frac{1}{\mu_H}\boldsymbol{\nabla}\phi = 0. \tag{1b}$$

For O^{+},

$$\frac{\partial \mathrm{n_O}}{\partial \mathrm{t}} + \boldsymbol{\nabla} \mathrm{n_O} \mathbf{u}_\mathrm{O} = 0, \tag{1c}$$

$$\frac{\partial \mathbf{u}_\mathrm{O}}{\partial \mathrm{t}} + (\mathbf{u}_\mathrm{O}.\boldsymbol{\nabla})\mathbf{u}_\mathrm{O} + \boldsymbol{\nabla}\phi = 0. \tag{1d}$$

For solar wind protons,

$$\frac{\partial \mathrm{n_{sp}}}{\partial \mathrm{t}} + \boldsymbol{\nabla} \mathrm{n_{sp}} \mathbf{u}_\mathrm{sp} = 0, \tag{1e}$$

$$\frac{\partial \mathbf{u}_\mathrm{sp}}{\partial \mathrm{t}} + \left(\mathbf{u}_\mathrm{sp}.\boldsymbol{\nabla}\right)\mathbf{u}_\mathrm{sp} + \frac{1}{\mu_{sp}}\boldsymbol{\nabla}\phi = 0. \tag{1f}$$

For Venusian electrons,

$$\mathrm{n_e} = \exp(\phi). \tag{1g}$$

For solar wind electrons,

$$\mathrm{n_{se}} = \exp\left(\frac{\phi}{\sigma_{se}}\right). \tag{1h}$$

Equations (1a)-(1h) are coupled through Poisson's equation:

$$\boldsymbol{\nabla}^2\phi = \gamma \mathrm{n_e} + \rho \mathrm{u_{se}} - \alpha \mathrm{n}_H - \mathrm{n}_O - \beta \mathrm{n}_{sp} = 0. \tag{1i}$$

In the above equations, the densities $\mathrm{n}_H, \mathrm{n}_O, \mathrm{n}_e, \mathrm{n}_{sp}$, and n_{se} are normalized by the unperturbed densities $\mathrm{n}_H^{(0)}, \mathrm{n}_O^{(0)}, \mathrm{n}_e^{(0)}, \mathrm{n}_{sp}^{(0)}$, and $\mathrm{n}_{se}^{(0)}$, respectively. Velocities $(\boldsymbol{u}_H, \boldsymbol{u}_O, \boldsymbol{u}_{sp})$ for hydrogen, oxygen, and solar wind protons are normalized by oxygen acoustic speed $C_s = (\frac{k_B T_{eff}}{m_O})^{1/2}$. ϕ is an electrostatic potential normalized by $(\frac{k_B T_{eff}}{e})$. Space and time variables can be normalized by: $\lambda_{Di} = (\frac{\epsilon_0\, k_B\, T_{eff}}{n_O e^2})^{1/2}$, and $\omega_{pi}^{-1} = (\frac{\epsilon_0\, m_O}{n_O^{(0)} e^2})^{1/2}$, respectively. Here k_B is the Boltzmann constant, e is the electron charge, T_{eff} is the effective temperature defined by $T_{eff} = \left[\frac{\gamma}{T_e} + \frac{\rho}{T_{se}}\right]^{-1}$, $\sigma_{se} = T_{se}/T_{eff}$ and T_e and T_{se} are the Venusian electron temperature and solar wind electron temperature.

The following ratios are used in the previous equations: $\mu_H = \mu_H/m_O$, which represents hydrogen to oxygen mass ratio, $\mu_{sp} = m_{sp}/m_O$ represents solar wind proton to oxygen mass ratio, $\alpha = n_H^{(0)}/n_O^{(0)}$ represents hydrogen to oxygen density ratio, $\gamma = n_e^{(0)}/n_O^{(0)}$ represents solar wind proton to oxygen density ratio, $\rho = n_{se}^{(0)}/n_O^{(0)}$ represents Venusian electron to oxygen density ratio, $\rho = n_{se}^{(0)}/n_O^{(0)}$ represents solar wind electron to oxygen density ratio.

To obtain the KP equation, we apply reductive perturbation analysis [19] to equations (1a)-(1i), establishing a weakly nonlinear theory for three-dimensional small but finite amplitude IAWs. Consequently, we scale the space and time variables in the standard form as follows:

$$\zeta = \epsilon^{\frac{1}{2}}(x - \lambda t), \tag{2a}$$

$$\eta = \epsilon y, \tag{2b}$$

$$\chi = \epsilon z, \tag{2c}$$

$$\tau = \epsilon^{3/2} t. \tag{2d}$$

Here, ϵ denotes a dimensionless expansion parameter quantifying the perturbation amplitude's magnitude, while λ is the phase velocity of IAWs along the x-axis normalized by C_s. Employing the reductive perturbation method involves expanding physical quantities like density, velocity, and potential around their equilibrium values as a power series of ϵ.

$$\begin{Bmatrix} n_H \\ u_{Hx} \\ u_{Hy} \\ u_{Hz} \\ n_O \\ u_{Ox} \\ u_{Oy} \\ u_{Oz} \\ n_{sp} \\ u_{spx} \\ u_{spy} \\ u_{spz} \\ n_e \\ n_{se} \\ \phi \end{Bmatrix} = \begin{Bmatrix} 1 \\ 0 \\ 0 \\ 0 \\ 1 \\ 0 \\ 0 \\ 0 \\ 1 \\ u_{spx}^{(0)} \\ 0 \\ 0 \\ 1 \\ 1 \\ 0 \end{Bmatrix} + \begin{Bmatrix} \epsilon n_H^{(1)} \\ \epsilon u_{Hx}^{(1)} \\ \epsilon^{3/2} u_{Hy}^{(1)} \\ \epsilon^{3/2} u_{Hz}^{(1)} \\ \epsilon n_O^{(1)} \\ \epsilon u_{Ox}^{(1)} \\ \epsilon^{3/2} u_{Oy}^{(1)} \\ \epsilon^{3/2} u_{Oz}^{(1)} \\ \epsilon n_{sp}^{(1)} \\ \epsilon u_{spx}^{(1)} \\ \epsilon^{3/2} u_{spy}^{(1)} \\ \epsilon^{3/2} u_{spz}^{(1)} \\ \epsilon n_e^{(1)} \\ \epsilon n_{se}^{(1)} \\ \epsilon \phi^{(1)} \end{Bmatrix} + \begin{Bmatrix} \epsilon^2 n_H^{(2)} \\ \epsilon^2 u_{Hx}^{(2)} \\ \epsilon^2 u_{Hy}^{(2)} \\ \epsilon^2 u_{Hz}^{(2)} \\ \epsilon^2 n_O^{(2)} \\ \epsilon^2 u_{Ox}^{(2)} \\ \epsilon^2 u_{Oy}^{(2)} \\ \epsilon^2 u_{Oz}^{(2)} \\ \epsilon^2 n_{sp}^{(2)} \\ \epsilon^2 u_{spx}^{(2)} \\ \epsilon^2 u_{spy}^{(2)} \\ \epsilon^2 u_{spz}^{(2)} \\ \epsilon^2 n_e^{(2)} \\ \epsilon^2 n_{se}^{(2)} \\ \epsilon^2 \phi^{(2)} \end{Bmatrix} + .., \tag{3}$$

The neutrality condition at equilibrium is satisfied by the relation

$$\gamma + \rho = \alpha + \beta + 1. \tag{4}$$

Using the stretching coordinates (2a)-(2d) and replacing the perturbed quantities (3) in the normalized fundamental equations (1a)-(1i) and then collecting terms of order (ϵ) from the continuity and momentum equations in the ζ-direction, we will obtain,

$$n_H{}^{(1)} = \frac{1}{\mu_H \lambda^2} \phi^{(1)}, \tag{5a}$$

$$u_{Hx}{}^{(1)} = \frac{1}{\mu_H \lambda} \phi^{(1)}, \tag{5b}$$

$$n_O{}^{(1)} = \frac{1}{\lambda^2} \phi^{(1)}, \tag{5c}$$

$$u_{Ox}{}^{(1)} = \frac{1}{\lambda} \phi^{(1)}, \tag{5d}$$

$$n_{sp}{}^{(1)} = \frac{1}{\mu_{sp} (\lambda - u_{spx}{}^{(0)})^2} \phi^{(1)}, \tag{5e}$$

$$u_{spx}{}^{(1)} = \frac{1}{\mu_{sp} (\lambda - u_{spx}{}^{(0)})} \phi^{(1)}, \tag{5f}$$

$$n_e{}^{(1)} = \phi^{(1)}, \tag{5g}$$

$$n_{se}{}^{(1)} = \frac{1}{\sigma_{se}} \phi^{(1)}. \tag{5h}$$

Upon gathering terms of order $\left(\epsilon^{3/2}\right)$ from the continuity and momentum equations along the η and χ directions, we will derive,

$$\frac{\partial u_{Hy}{}^{(1)}}{\partial \zeta} = \frac{1}{\mu_H \lambda} \frac{\partial \phi^{(1)}}{\partial \eta}, \tag{6a}$$

$$\frac{\partial u_{Hz}{}^{(1)}}{\partial \zeta} = \frac{1}{\mu_H \lambda} \frac{\partial \phi^{(1)}}{\partial \chi}, \tag{6b}$$

$$\frac{\partial u_{Oy}{}^{(1)}}{\partial \zeta} = \frac{1}{\lambda} \frac{\partial \phi^{(1)}}{\partial \eta}, \tag{6c}$$

$$\frac{\partial u_{Oz}{}^{(1)}}{\partial \zeta} = \frac{1}{\lambda} \frac{\partial \phi^{(1)}}{\partial \chi}, \tag{6d}$$

$$\frac{\partial u_{spy}{}^{(1)}}{\partial \zeta} = \frac{1}{\mu_{sp}\left(\lambda - u_{spx}{}^{(0)}\right)} \frac{\partial \phi^{(1)}}{\partial \eta}, \tag{6e}$$

$$\frac{\partial u_{spz}{}^{(1)}}{\partial \zeta} = \frac{1}{\mu_{sp}\left(\lambda - u_{spx}{}^{(0)}\right)} \frac{\partial \phi^{(1)}}{\partial \chi}. \tag{6f}$$

The Poisson's equation's lowest order of (ϵ) terms yields

$$\frac{\alpha}{\mu_H \lambda^2} + \frac{1}{\lambda^2} + \frac{\beta}{\mu_{sp}\left(\lambda - u_{spx}^{(0)}\right)^2} - \gamma - \frac{\rho}{\sigma_{se}} = 0. \tag{7}$$

The compatibility condition governing our plasma system is represented by equation (7), which is a mathematical tool that is essential for figuring out the phase velocity of the IAWs.

We obtain formulations for the second-order perturbed densities by solving the resulting system of equations (6a)-(6f) using the first-order equations (5a)-(5h). We eventually obtain the Kadomtsev–Petviashvili (KP) nonlinear partial differential equation.

$$\frac{\partial}{\partial \zeta}\left(\frac{\partial \phi}{\partial \tau} + A\phi \frac{\partial \phi}{\partial \zeta} + B\frac{\partial^3 \phi}{\partial \zeta^3}\right) + C\left(\frac{\partial^2 \phi}{\partial \eta^2} + \frac{\partial^2 \phi}{\partial \chi^2}\right) = 0. \tag{8}$$

From now on, we shall use ϕ instead of $\phi^{(1)}$ for simplicity's sake. Additionally, the system's nonlinear, dispersive, and dispersion coefficients A, B, and C are defined as follows, in that order:

$$A = B\left(\frac{3\alpha}{\mu_H^2 \lambda^4} + \frac{3}{\lambda^4} + \frac{3\beta}{\mu_{sp}^2\left(\lambda - u_{spx}^{(0)}\right)^4} - \gamma - \frac{\rho}{\sigma_{se}^2}\right), \tag{9}$$

$$B = \left(\frac{2\alpha}{\mu_H \lambda^3} + \frac{2}{\lambda^3} + \frac{2\beta}{\mu_{sp}\left(\lambda - u_{spx}^{(0)}\right)^3}\right)^{-1}, \tag{10}$$

$$C = B\left(\frac{\alpha}{\mu_H \lambda^2} + \frac{1}{\lambda^2} + \frac{\beta}{\mu_{sp}\left(\lambda - u_{spx}^{(0)}\right)^2}\right). \tag{11}$$

The KP equation governs the development of the fundamental approximation of electrostatic potential, which is associated with ion-acoustic waves (IAWs) in plasma. When transverse perturbations are factored in, an extra term appears in equation (8), converting it into the classical Korteweg–de Vries (KdV) equation in the absence of transverse perturbations. Consequently, the presence of transverse perturbations has the potential to modify the features of IAW structures.

3. Mathematical solution and discussion

Since equation (8) includes the lowest-order nonlinearity and dispersion, it can only be used to describe small but finite amplitude waves. The breakdown of a soliton is indicated by a deviation in its width and velocity from the KP equation as the wave amplitude increases. Higher-order nonlinear and dispersive effects need to be taken into account in order to appropriately characterize solitons with larger amplitudes [20]. For this, the reductive perturbation method's higher-order approximation is a useful tool. However, this study is not intended to address these higher-order effects.

To obtain the soliton solution of (8), we introduce the traveling-wave transformation,

$$\xi = L_1\zeta + L_2\eta + L_3\chi - U\tau, \tag{12}$$

where ξ represents the transformed coordinates in a frame moving with velocity U. L_1, L_2 and L_3 are the directional cosines of the wave vector k along the ζ, η and χ axes, respectively, satisfying the relation $L_1^2 + L_2^2 + L_3^2 = 1$. Integrating (8) with respect to the variable ξ and applying the vanishing boundary condition for ϕ and its derivatives up to the second order as $|\xi| \to \infty$, yields

$$\frac{d^2\phi}{d\xi^2} = \frac{h}{BL_1^4}\phi - \frac{A}{2BL_1^2}\phi^2. \tag{13}$$

The one-soliton solution of equation (13) is given by,

$$\phi = \phi^{(0)} sech^2(\xi\omega), \tag{14}$$

where $\phi^{(0)} = 3h/AL_1^2$ is the amplitude of the soliton, $\omega = \sqrt{\frac{4BL_1^2}{h}}$ is the width of soliton and $h = L_1U - C(1 - L_1^2)$.

We will use an energy-based approach to evaluate whether a given plasma equilibrium is stable or unstable. Using this method, the change in the plasma's potential energy as a result of a known perturbation is calculated. This approach yields the potential energy, which is commonly known as the Sagdeev potential [21] . Integrate equation (13) to yield the nonlinear equation of motion as

$$\frac{1}{2}\left(\frac{d\phi}{d\xi}\right)^2 + V(\phi) = 0, \tag{15}$$

where the Sagdeev potential $V(\phi)$ is given by

$$V(\phi) = \frac{A}{6BL_1^2}\phi^3 - \frac{h}{2BL_1^4}\phi^2. \tag{16}$$

A necessary condition for the existence of solitary waves is

$$d^2V(\phi)/d\phi^2 < 0 \text{ for } \phi = 0. \tag{17}$$

A value of $d^2V(\phi)/d\phi^2$ greater than zero predicts the formation of a shock in the plasma. From (16) and (17) we obtain

$$\frac{d^2V(\phi)}{d\phi^2} = \frac{-h}{BL_1^4}. \tag{18}$$

Equation (18) shows that stable solitons will exist when $\frac{-h}{BL_1^4} > 0$, otherwise stable solitons do not exist in the plasma. It is clear that B and L_1 are greater than zero but h may be less than zero.

We will study the IAWs numerically in a homogeneous, unmagnetized, collisionless plasma using data from the VEX Noon-Midnight (NM) meridian and PVO missions to make sure our results have physical significance. In light of transverse perturbations, our goal is to examine the effects of these factors on the propagation of IAWs in the Venusian ionosphere at altitudes ranging from 10^3 to 10^4 km. Examining the behavior of the phase velocity λ and how it relates to physical quantities like the temperature ratio σ_{se} is enlightening.

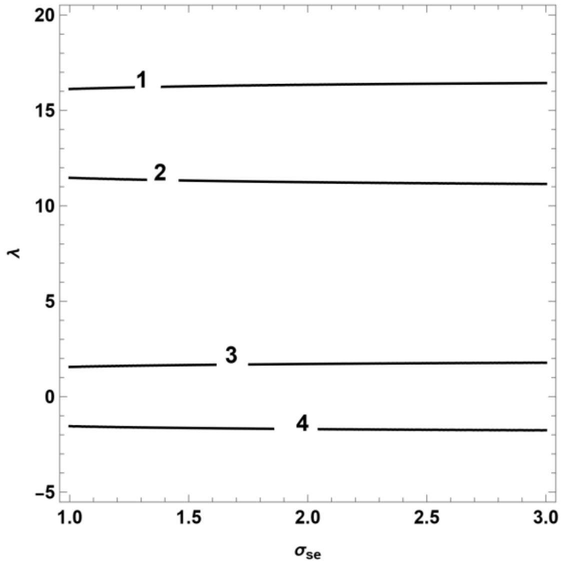

Figure 1: The phase velocity λ versus the temperature ratio $\sigma_{se} = \left(T_{se}/T_{eff}\right)$ is presented using parameter values $\mu_H = \mu_{sp} = 0.0625$, $U = 0.1$, $\gamma = 1 + \alpha + \beta - \rho$, $\alpha = 0.2$, $\beta = \rho = 0.6$, and $u_{sp}^{(0)} = 13.8$.

To gain insights into the phase velocity λ of our nonlinear structures, we modified the compatibility condition (7) to form a fourth-order polynomial in λ. We then solved this polynomial numerically, yielding four distinct roots. Each root corresponds to a possible mode with a specific phase velocity. These four roots are depicted in figure (1) plotted against the relative temperature $\sigma_{se} = \left(T_{se}/T_{eff}\right)$. Figure (1) illustrates that there are four ion-acoustic modes, labeled as λ_{1-4}, where it is clear that λ is supersonic (i.e., (λ>1)). Also, it is seen that $\lambda_{1,2,3}$ are forward (i.e., have a positive value) and λ_4 is backward (i.e., has a negative value). Consequently, we focus on the region where λ is positive. It is important to mention here that in our following calculations we use the third root of λ (i.e., λ_3) since it is coincident with the space observations.

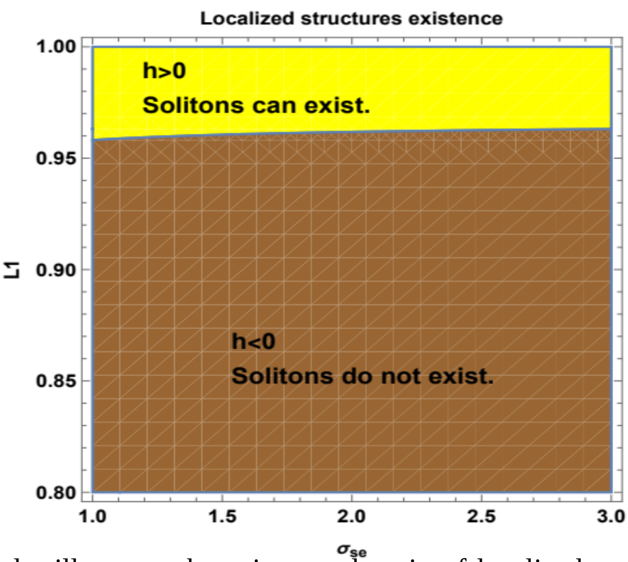

Figure 2: The region plot illustrates the existence domain of localized structures solutions based on the direction cosine L_1 and temperature ratio $\sigma_{se} = \left(T_{se}/T_{eff}\right)$, with parameters $\mu_H = \mu_{sp} = 0.0625$, $U = 0.1$, $L_1 = 0.96$, $L_2 = 0.15$, $L_3 = \sqrt{1 - L_1^2 - L_2^2}$, $\alpha = 0.2$, $\beta = \rho = 0.6$, and $u_{sp}^{(0)} = 13.8$.

Figure (2) depicts the existence domain as a function of the direction cosine L_1 and the temperature ratio σ_{se}. This domain is divided into two regions: yellow zones where $(h > 0)$ localized pulses can exist, and brown zones where $(h < 0)$ localized pulses cannot propagate. According to condition $\frac{h}{BL_1^4}$, we can conclude that localized solitary waves can exist for $L_1 > 0.96$. One can conclude that the solitary wave in our system can propagate only in the quasi-parallel case. In the quasi-parallel case, we set L_2 and L_3 to very low values (i.e., $L_{2,3} \geq 0$). Hence, for a localized pulse (solitary wave) to exist, the transverse perturbation should be weak. Otherwise, it cannot propagate, and other nonlinear structures may occur, but they are outside the scope of the present work and will be considered in our future work.

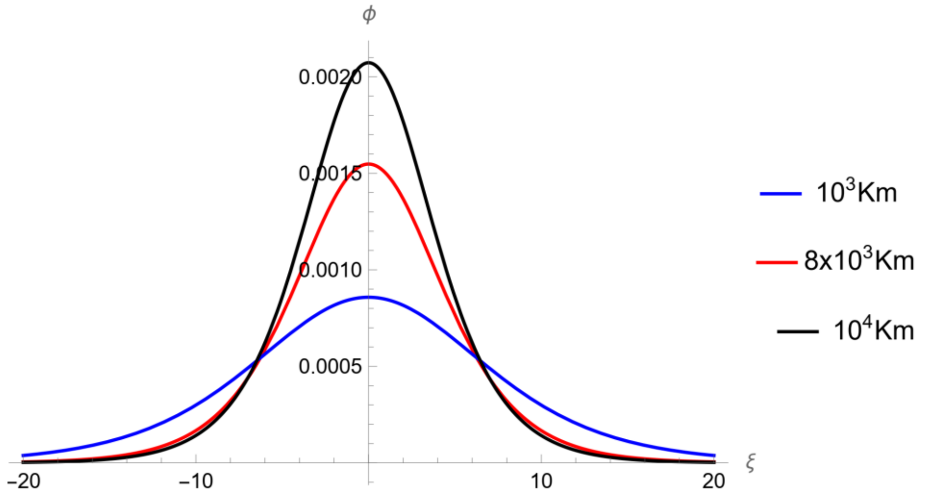

Figure 3: The effect of altitude on the solitary pulses against ξ at $\mu_H = \mu_{sp} = 0.0625$, and $U = 0.6$, $L_1 = 0.96$, $L_2 = 0.15$, $L_3 = \sqrt{1 - L_1^2 - L_2^2}$ at altitude of 10^3 km, where $\alpha = 0.2$, $\beta = \rho = 0.6$, $u_{sp}^{(0)} = 13.8$, $\sigma_{se} = 1$, at 8x10^3 km, where $\alpha = 0.3$, $\beta = \rho = 0.55$, $u_{sp}^{(0)} = 16.6$, at 10^4 km, with $\alpha = 0.4$, $\beta = \rho = 0.5$, $u_{sp}^{(0)} = 20.8$, and $\sigma_{se} = 3$

Figure (3) illustrates that at different altitudes, the localized pulse profile changes due to changes in plasma physical parameters. At higher altitudes, the amplitude of the solitary wave increases, but the width decreases. This can be explained by the fact that at high altitudes, the system receives energy from the streaming particles coming from the solar wind, which causes the amplitude to be taller. As we descend into the lower layers of the atmosphere, the density of the streaming particles decreases, and the pumped energy into the plasma decreases, resulting in a dwarfed pulse profile.

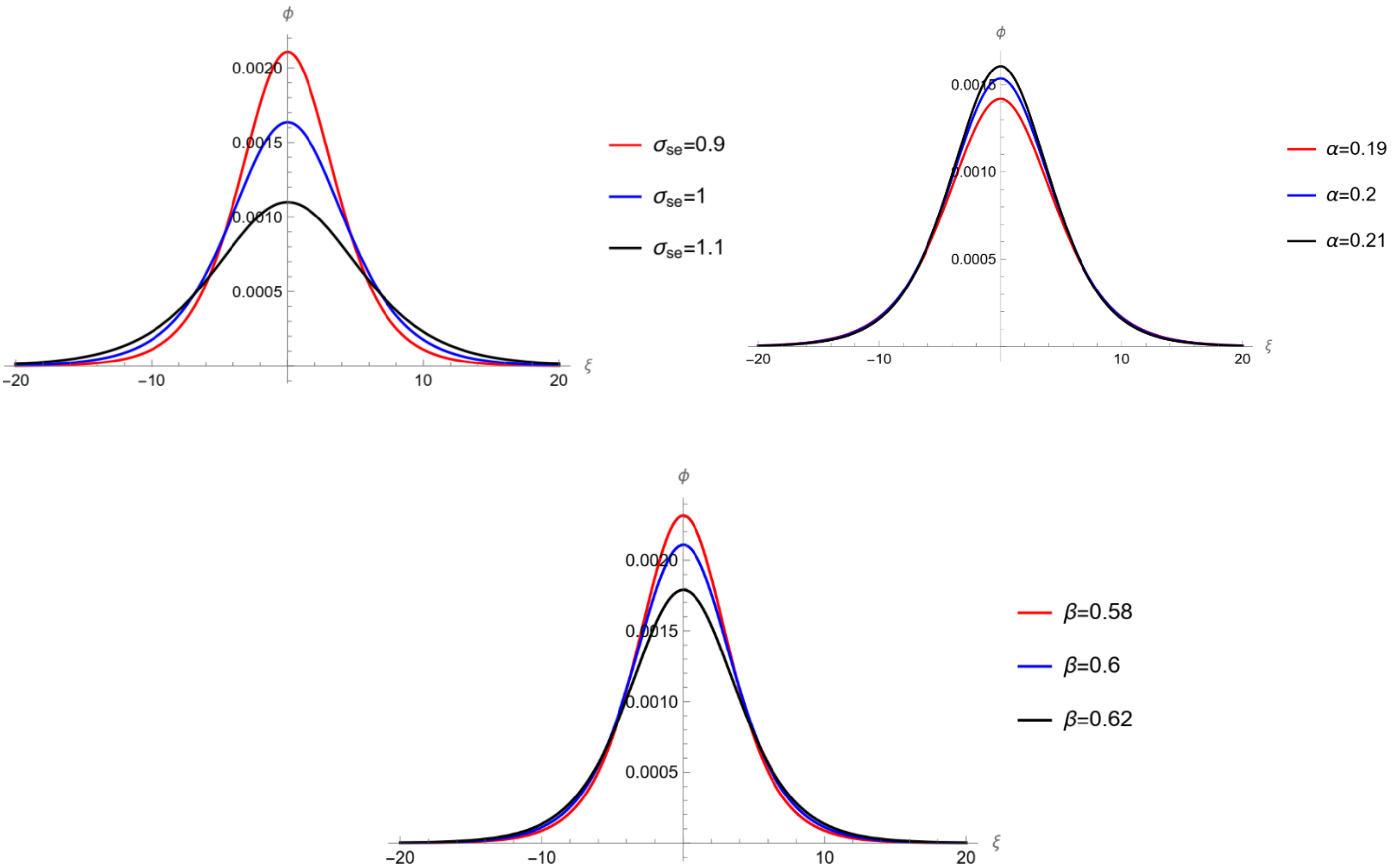

Figure 4: Profiles of solitary waves against ξ at altitude 10^3 Km where, μ_H (= m_H/m_O) = μ_{sp} (= m_{sp}/m_O) = 0.0625, U=0.1, L_1 = 0.96, L_2 = 0.15, $L_3 = \sqrt{1 - L_1^2 - L_2^2}$, γ (= $n_e^{(0)}/n_O^{(0)}$) = 1 + α + β - ρ, $u_{sp}^{(0)}$ = 13.8, where: (a) profiles in dependence on σ_{se} (= T_{se}/T_e) where, α (= $n_H^{(0)}/n_O^{(0)}$)=0.2, β (= $n_{sp}^{(0)}$ /$n_O^{(0)}$) = ρ (= $n_{se}^{(0)}/n_O^{(0)}$)=0.6, (b) profiles in dependence on α, where β=ρ=0.6, σse=1. (c) profiles in dependence on β, where α=0.2, ρ=0.6, σse=1.

In figure (4), we investigate the effect of various physical parameters σ_{se}, α, and β on solitary waves. We examine the effect of the relative temperature $\sigma_{se} = \left(T_{se}/T_{eff}\right)$ on solitary structures in figure 4(a), increasing relative temperature σ_{se} considerably reduces the amplitude of the solitary pulse while slightly increasing its spatial coordinate, as shown in figure 4(a). This indicates that as the temperature of electrons increases, the energy of positive soliton pulses will decrease. Figure 4(b) illustrates that higher relative density $\alpha\left(= n_H^{(0)}/n_O^{(0)}\right)$ values increase the amplitude of the solitary pulse and decrease its width, which means that higher α values enhance the nonlinearity of the wave structures, also the density $\alpha\left(= n_H^{(0)}/n_O^{(0)}\right)$ of the positive component H^+ will increase with altitude, as shown in 4(b), which will cause the streaming protons to pump energy into the system. Lower relative density $\beta\left(= n_{sp}^{(0)}/n_O^{(0)}\right)$ values increase the nonlinearity of the wave structures as shown in 4(c) as increasing β values, decreases the amplitude and increase the width of the pulse. It indicates that the system is getting energy from the solar wind particles that are flowing across it. A balance between nonlinearity and dispersion in the medium leads to the occurrence of solitons. Eventually, when the amplitude increases, the width decreases, and vice versa, due to the ability of solitons to maintain their shape over long distances.

4. Summary

In summary, we studied the basic features of solitary waves in an unmagnetized, homogeneous, collisionless plasma system consisting of two positively charged planetary ions (H^+ and O^+) and electrons as long as solar wind protons and electrons. Reductive perturbation analysis has been used to obtain the three-dimensional KP equation, which describes the propagation of the IAWs at altitudes of ($10^3 - 10^4$) km in the Venusian ionosphere. The Sagdeev potential was calculated using an energy-based approach. The conclusions derived from our work can be summed up as follows:

(i) We investigated the four roots of λ in relation to the relative temperature $\sigma_{se} = \left(T_{se}/T_{eff}\right)$. Our findings indicate the existence of four ion-acoustic modes, λ_{1-4}, where phase velocity is supersonic (λ>1). Furthermore, it can be observed that $\lambda_{1,2,3}$ is inward that is, it has a positive value while λ_4 is backward that is, it has a negative value. As a result, the region where λ is positive is our main concern. Note that because λ_3 coincides with the space observations, we used the third root of λ in our calculations.

(ii) It is found that the direction cosine L_1 parameter influences the occurrence of soliton pluses more than any other physical parameter. For $L_1 > 0.96$, it can be concluded that solitary wave exists only for quasi-parallel propagation.

(iii) We found that the energy pumped into the system by solar wind particles causes these solitary wave pulses to become taller at higher altitudes.

(iv) We studied the effects of relative temperature σ_{se} and relative densities α, and β on solitary waves. Increasing σ_{se} reduces the amplitude and slightly increases the spatial size of solitary pulses, suggesting that the energy of positive soliton pulses decreases as electron temperatures increase. Higher α values increase the amplitude and decrease the width, indicating that greater α values enhance wave structures' nonlinearity. Conversely, increasing β decreases the amplitude and increases the width, implying that the system is energized by solar wind particles, with a balance between nonlinearity and dispersion leading to solitons.

(iv) As the effective temperature increases, the energy of the solitary pulses decreases, resulting in a shorter amplitude. Increasing α and β implies that the number density of the oxygen ions decreases. This reduces the charged moving ions and increases the energy per ion gained from the solar wind ions. This increases the total energy of the moving ions in our time-scale phenomena, resulting in a taller amplitude.

5. REFERENCES

[1] M. A. Belyaev, D. J. Larson, B. I. Cohen, and S. E. Clark, “Topanga: A kinetic ion plasma code for large-scale ionospheric simulations on magnetohydrodynamic timescales,” Physics of Plasmas, vol. 31, no. 1, 2024. [Online]. Available: https://pubs.aip.org/aip/pop/article/31/1/012902/3051553

[2] B. Goldstein, The Solar Wind. American Geophysical Union (AGU), 1998, pp. 73–79. [Online]. Available: https://agupubs.onlinelibrary.wiley.com/doi/abs/10.1029/ SP050p0073

[3] N. El-Shafeay, W. Moslem, W. El-Taibany, and S. El-Labany, “Role of solar wind on the ionic escaping from venus upper ionosphere via plasma wakefield,” Physica Scripta, vol. 98, no. 3, p. 035603, 2023.

[4] S. Salem, W. Moslem, M. Lazar, R. Sabry, R. Tolba, and R. Schlickeiser, “Ionospheric losses of venus in the solar wind,” Advances in Space Research, vol. 65, no. 1, pp. 129–137, 2020. [Online]. Available: https://www.sciencedirect.com/science/article/abs/ pii/S0273117719307100

[5] N. Meyer-Vernet, Basics of the solar wind. Cambridge University Press, 2007

[6] F. W. Taylor, “Venus before venus express,” Planetary and Space Science, vol. 54, no. 13, pp. 1249–1262, 2006, the Planet Venus and the Venus Express Mission. [Online]. Available: https://www.sciencedirect.com/science/article/pii/S0032063306001553

[7] J. L. Phillips and D. J. McComas, “The magnetosheath and magnetotail of venus,” Space Science Reviews,vol.55,no.1,pp.1–80,1991.[Online].Available: https://link.springer.com/article/10.1007/BF00177135

[8] C. Russell and O. Vaisberg, “The interaction of the solar wind with venus,” in Venus, 1983, pp. 873–940. [Online]. Available: https://www.elibrary.ru/item.asp?id=24378108

[9] E. Dubinin, J. G. Luhmann, and J. A. Slavin, “Solar wind and terrestrial planets,” 06 2020. [Online]. Available:https://oxfordre.com/planetaryscience/view/10.1093/ acrefore/9780190647926.001.0001/acrefore-9780190647926-e-184

[10] G. L. Siscoe and J. A. Slavin, “Planetary magnetospheres,” Reviews of Geophysics, vol. 17, no. 7, pp.1677–1693,1979. [Online].Available:https://agupubs.onlinelibrary. wiley.com/doi/abs/10.1029/RG017i007p01677

[11] J. Slavin, R. Holzer, J. Spreiter, S. Stahara, and D. Chaussee, “Solar wind flow about the terrestrial planets: 2. comparison with gas dynamic theory and implications for solar-planetary interactions,” Journal of Geophysical Research: 12 AJBAS Volume VV, Issue II, 2024 Space Physics, vol. 88, no. A1,pp.19–35,1983.

[12] V. K. Yadav, “Plasma waves around venus and mars,” IETE Technical Review, vol. 38, no. 6, pp. 622–661, 2021.

[13] R. Lundin, S. Barabash, Y. Futaana, J.-A. Sauvaud, A. Fedorov, and H. Perez-de Tejada, “Ion flow and momentum transfer in the venus plasma environment,” Icarus, vol. 215, no. 2, pp. 751–758, 2011.

[14] W. C. Knudsen, “The venus ionosphere from in situ measurements.” Geophysical Monograph Series, vol. 66, pp. 237–263, 1992.

[15] K. Mahajan and A. Dwivedi, “Ionospheres of venus and mars: a comparative study,” Advances in Space Research, vol. 33, no. 2, pp. 145–151, 2004.

[16] S. Tsang, A. J. Coates, G. H. Jones, R. Frahm, J. Winningham, S. Barabash, R. Lundin, and A. Fedorov, “Ionospheric photoelectrons at venus: Case studies and first observation in the tail,”Planetary and Space Science, vol. 113, pp. 385–394, 2015. [Online]. Available: https://www.sciencedirect.com/science/article/pii/S0032063315000203?via%3Dihub

[17] S. El-Labany, W. M. Moslem, W. El-Taibany, and M. Mahmoud, “Kadomtsevpetviashvili equation for dust acoustic solitary waves in a warm dusty plasma with dust charge variation,” Physica Scripta, vol. 70, no. 5, p. 317, 2004.

[18] M. Afify, I. Elkamash, M. Shihab, and W. Moslem, “Evolution of ion-acoustic soliton waves in venus’s ionosphere permeated by the solar wind,” Advances in Space Research, vol. 67, no. 12, pp. 4110–4120, 2021.

[19] H. Washimi and T. Taniuti, “Propagation of ion-acoustic solitary waves of small amplitude,” Physical Review Letters, vol. 17, no. 19, p. 996, 1966.

[20] M. J. Ablowitz and H. Segur, Solitons and the inverse scattering transform. SIAM, 1981. [Online]. Available: https://apps.dtic.mil/sti/tr/pdf/ADA088023.pdf

[21] N. A. Krall, A. W. Trivelpiece, and R. A. Gross, “Principles of Plasma Physics,” American Journal of Physics, vol. 41, no. 12, pp. 1380–1381, 12 1973